LBL-21433
UC-21

Lawrence Berkeley Laboratory
UNIVERSITY OF CALIFORNIA

RECEIVED
LAWRENCE
BERKELEY LABORATORY

JUL 2 1986

LIBRARY AND
DOCUMENTS SECTION

Accelerator & Fusion Research Division

HEAVY ION FUSION ACCELERATOR RESEARCH (HIFAR)
HALF-YEAR REPORT: October 1, 1985-March 31, 1986

Heavy Ion Fusion Staff

May 1986

TWO-WEEK LOAN COPY
This is a Library Circulating Copy
which may be borrowed for two weeks

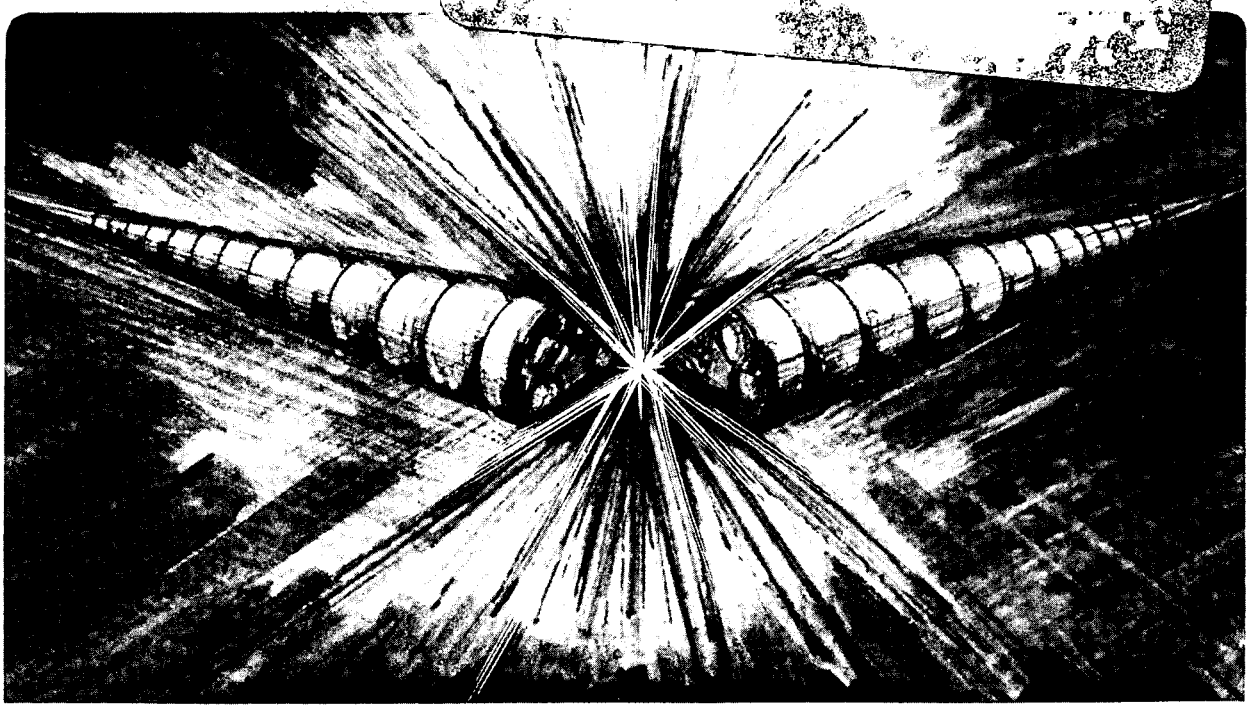

Prepared for the U.S. Department of Energy under Contract DE-AC03-76SF00098

LBL-21433 c.2

DISCLAIMER

This document was prepared as an account of work sponsored by the United States Government. While this document is believed to contain correct information, neither the United States Government nor any agency thereof, nor the Regents of the University of California, nor any of their employees, makes any warranty, express or implied, or assumes any legal responsibility for the accuracy, completeness, or usefulness of any information, apparatus, product, or process disclosed, or represents that its use would not infringe privately owned rights. Reference herein to any specific commercial product, process, or service by its trade name, trademark, manufacturer, or otherwise, does not necessarily constitute or imply its endorsement, recommendation, or favoring by the United States Government or any agency thereof, or the Regents of the University of California. The views and opinions of authors expressed herein do not necessarily state or reflect those of the United States Government or any agency thereof or the Regents of the University of California.

LBL-21433
HIFAN-312

HEAVY ION FUSION ACCELERATOR RESEARCH (HIFAR) HALF-YEAR REPORT*

October 1, 1985 - March 31, 1986

Heavy Ion Fusion Staff

Accelerator and Fusion Research

Lawrence Berkeley Laboratory
University of California
Berkeley, CA 94720

May 1986

Attention: This document is provided for DOE "Official Use". Distribution to other interested parties is made with the understanding that no information or experimental results given herein will be quoted without first obtaining the authors' permission, or until such information or results have appeared in the open literature.

*This work was supported by the Office of Energy Research, Office of Basic Energy Sciences, U.S. Department of Energy under Contract No. DE-AC03-76SF00098.

FOREWORD

The basic objective of the Heavy Ion Fusion Accelerator Research (HIFAR) program is to assess the suitability of heavy ion beam accelerators as igniters for Inertial Confinement Fusion (ICF). A specific accelerator technology, the induction linac, has been studied at the Lawrence Berkeley Laboratory and has reached the point at which its viability for ICF applications can be assessed over the next few years.

The HIFAR program addresses the generation of high-power, high-brightness beams of heavy ions, the understanding of the scaling laws in this novel physics regime, and the validation of new accelerator strategies, to cut costs. Key elements to be addressed include: 1) Beam quality limits set by transverse and longitudinal beam physics; 2) Development of induction accelerating modules, and multiple beam hardware, at affordable costs; 3) Acceleration of multiple beams with current amplification -- both new features in a linac -- without significant dilution of the optical quality of the beams; 4) Final bunching, transport, and accurate focussing on a small target.

TABLE OF CONTENTS

	Page
HIGHLIGHTS	1
STATUS OF MBE-4 APPARATUS	4
ACCELERATION AND ENVELOPE OSCILLATIONS IN MBE-4	5
TRANSVERSE BEAM DYNAMICS	6
NEW DIRECTIONS FOR HIF DRIVERS	7
IDENTIFICATION OF ISSUES PERTAINING TO MERGING AND EXPLORATION OF THE MULTIPLE-BEAM PARAMETER SPACE	8
MULTIPLE PULSING OF INDUCTION LINACS	10
MBE-4 QUADRUPOLE INSULATOR TESTS	11
PUBLICATIONS AND INTERNAL NOTES	12
HIF STAFF ROSTER	16
DISTRIBUTION LIST	17

HIGHLIGHTS

D. Keefe

(1) The first two accelerating sections (A and B) of the six-section MBE-4 experiment have been installed and operated. A major activity during this period that been the development of pulsers for the eight accelerating units in Sections A and B; these have now been built and adjusted to supply the right waveforms to initiate the current-amplification process.

Simultaneous acceleration and current amplification of the four cesium beams has been experimentally tested.

(2) The velocity tilt from head-to-tail of the beam bunch, which inevitably occurs in the process of current amplification, gives rise to a variation in the transverse beam dynamics along the length of the bunch. This effect, together with the change in energy as the particles traverse the accelerating gaps, has now been incorporated in the envelope computer codes and the results found to agree with experiment.

(3) The conceptual design of the low-voltage section of a driver accelerator has received increasing attention in this period. (Usually, the linac design code LIACEP examines designs only above the 50 MV point -- precisely to avoid the special design problems at the low voltage end.) An economically attractive strategy seems to be to start with a rather large number of beams (perhaps 50 to 100) from the injector and, after some acceleration, to merge them to a smaller number (perhaps 16) for acceleration to final energy and delivery to the target.

(4) Interest in using heavy ions with charge state, q, greater than unity has been revived as a result of the significant cost saving indicated by the ongoing HIF Systems Assessment and, also, by emergence of a source (MEVVA) that may be able to supply large currents at $q > 1$. The optimum charge state seems to be $q = 3$ for $A = 200$; charge states higher than this may require an excessive number of beams on target.

While the front end (< 50 MV) of a driver accounts for only about 10% of the cost of a driver with an ion of $q = 1$, it represents a larger fraction for ions with $q = 3$ and, accordingly, deserves more attention than it has previously merited. Low-energy end becomes even greater when one considers ions with $q > 1$ if they are to be transported by electric quadrupoles.

(5) PIC simulations of an intense beam with a non-uniform density distribution in configuration space confirm the calculations by Anderson (Particle Accelerators, to be published) that a persistent plasma oscillation is set up if the perturbation is moderate, but that emittance growth occurs if it is large.

Simulations also predict that merging of space-charge dominated beams will result in a larger emittance growth, therefore, than one would calculate traditionally by examining the initial emittance dilution in phase-space alone.

(6) Successful double pulsing of induction cores with rapid reset between pulses has now been demonstrated.

Double- or multiple-pulsing an induction linac with a short interval (~ 10 μsec) between pulses may have cost advantages for a driver. Double pulsing a 1 MJ, driver with $q = 1$ ions, to give 2 MJ on target will save more in the cost of the structure than is paid for the extra pulsers; the cost advantage, if any, for $q = 3$ ions is not yet established. Independent of savings, however, multiple

pulsing may provide an attractive strategy for a first test driver in that one could begin with a 0.5 MJ driver, and advance its capabilities to 1, 1.5, 2 MJ in successive stages of multiple pulsing as needed.

STATUS OF MBE-4 APPARATUS

A. I. Warwick, D. Vanecek, and D. Brodzik
(on behalf of the MBE-4 Team)

During the first half of FY86 two beam focussing assemblies for accelerator sections B & C and four core assemblies, one for each of the four accelerating gaps in accelerator section B were fabricated. The assembly and installation of accelerator section B was complete in November. The five quadrupole doublets with four induction insulators are positioned within an accuracy of .003" RMS. For details of these measurements see year end report for FY85. Figure 1 illustrates the present mechanical arrangement of the whole system.

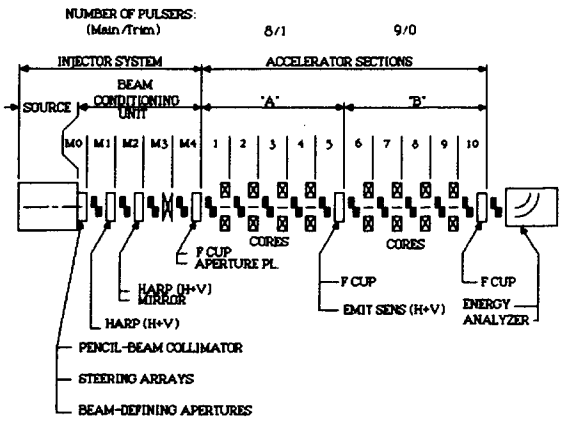

XBL 864-1527

Fig. 1. Components installed on MBE-4 at the end of March 1986.

The arrangement of the core assembly for section B is shown in Fig. 2. The individual core packages are similar to those used in accelerator section A. They contain Astron cores, as used in section A, and larger silicon-steel cores, wound from .002 inch thick x 1.40 inch wide ribbon. The individual silicon-steel cores are packaged in the same way as the individual Astron cores. The Astron triple core package has been modified; there are no corner cuffs at the two inner core corners, as shown in Fig. 3, and an insulator spacer .375" thick has been added between each core package.

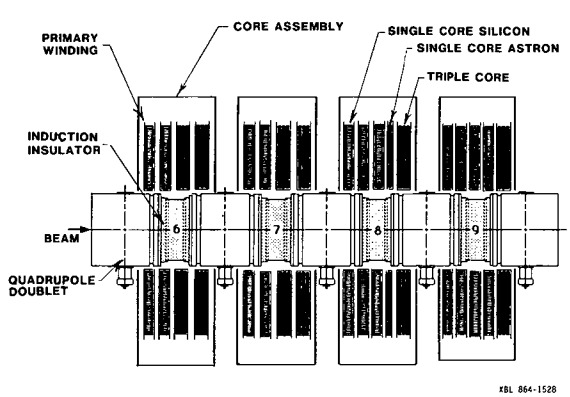

Fig. 2. Arrangement of cores for accelerator section B

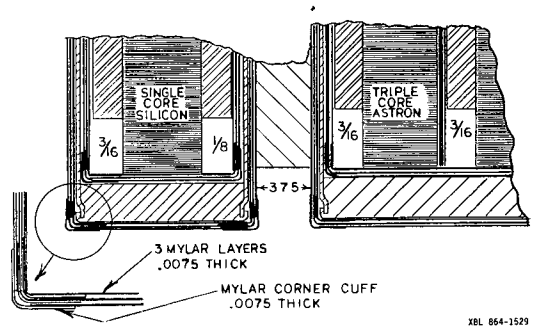

Fig. 3. Core insulation details

The beam focussing assembly for accelerator section C was to be installed in mid-March, but due to out-of-tolerance positioning of the five quadrupole doublets and the four induction insulators, the unit could not be installed at this time. The quality control and assembly procedures are being re-evaluated and upgraded. The beam focussing assembly for accelerator section C is scheduled to be re-assembled by mid-April.

March 1986 saw a full complement of pulsers tuned and operational on accelerating section A. This includes a trim pulser on gap 4 to control longitudinal space charge effects in the tail of the bunch. Figure 4 shows the three pulsers on gap 4 tuned to amplify the beam current as $\beta^{1.3}$; pulser 3 is the space charge trim. The first control of the space charge at the head of the bunch will be applied in the very near future at gap 6.

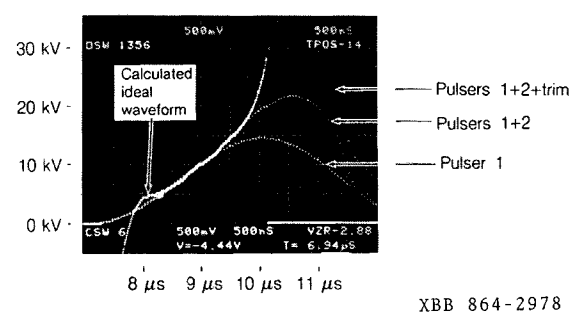

Fig. 4. Calculated design accelerating waveform compared to actual waveforms on gap 4

Pulsers for section B are now installed and ready for first operation. These drive a combination of nickel-iron Astron cores (6.8 mVs) and silicon-steel cores (23.9 mVs). The section B pulsers produce composite waveforms rising to 20 kV in times of the order of 0.5 μs then to 30 kV in a further 2.4 μs. Circuits are designed by modelling the cores as resistors; 5 for the Astron cores and 8 for the silicon-steel cores.

ACCELERATION AND ENVELOPE OSCILLATIONS IN MBE-4

A.I. Warwick and C.H. Kim

Pulsers are now operational on the four gaps of section A of MBE-4, and we have begun to study the coupling between longitudinal and transverse beam dynamics during acceleration.

The longitudinal dynamics is prescribed by a calculated acceleration and current-amplification schedule. This calculation specifies the current and kinetic energy as a function of position in the bunch in such a way that as the beam is accelerated the current is amplified with a waveform that retains the initial shape. (The current waveform is the time dependent current as measured at a fixed location). This is called current self replication and the preferred current waveform is flat (1). The calculation also specifies the accelerating voltage waveforms to be applied to each gap. These waveforms include the corrections necessary to control the longitudinal space charge forces at the bunch ends. The specified voltage waveforms are written from the computer to the screen of a digital oscilloscope where they can be directly compared with the actual waveforms on the accelerating gaps. By this means the longitudinal dynamics of MBE-4 can be precisely tuned. The results of this procedure agree closely with the original calculation (2).

The longitudinal and transverse dynamics are coupled. The kinetic energy varies through the length of the bunch so that the kinetic energy of the head is different to that of the tail as they pass a given point in the accelerator. Since the quadrupole voltages are constant, the transverse dynamics vary from head to tail.

The matching section of MBE-4 is tuned to introduce the beams into the first accelerating gap with envelopes matched for transport at $\sigma_0 = 60°$ with a kinetic energy of 200 keV. Once acceleration begins it is impossible to maintain the matched conditions for the entire bunch. One is free to choose quadrupole voltages to minimise the induced envelope oscillations, provided σ_0 does not move outside the desired range of values either for the head or the tail.

In order to study the envelope oscillations induced during acceleration it is necessary to interpolate the behavior of the envelopes between the diagnostic stations which are five quadrupole periods apart. Provided that the non-linear part of the space charge force is not too large, the K-V envelopes will be accurate enough. That this is so is seen in Fig. 1. The upper part of the figure shows an integration of the K-V envelope equations through five periods. The initial conditions are twice the measured r.m.s. radii and divergences in the first diagnostic box.

$$2\sqrt{\langle x^2 \rangle} \quad \text{and} \quad 2\sqrt{\langle x'^2 \rangle}$$

Acceleration is applied suddenly at the centre of each accelerating gap and the current increases according to the acceleration schedule. The quadrupole strengths are set to maintain the middle of the bunch at $\sigma_0 = 60°$. In the lower part of the figure the horizontal phase space distributions, measured after five periods at the second diagnostic box (gap 5, at the end of section A) for the head and tail of the bunch, are compared to the corresponding K-V ellipses. Agreement is good and the calculation reproduces the difference between the optics of the head and the tail.

The K-V envelope equations can therefore be used to analyse the envelope oscillations induced by acceleration. Figure 2 shows an integration through fifteen quadrupole periods of the envelopes of the middle of the bunch. The initial conditions are again the measured values and the first five periods reproduce the actual acceleration in section A. In the subsequent ten periods the kinetic energy,current and quadrupole strength are constant and the developed envelope oscillation can be seen. During the first five periods the quadrupole strength is increasing to maintain $\sigma_0 = 60°$ for the middle of the bunch. The current is amplified like $\beta^{1.3}$ in this example so that the perveance decreases and an oscillation develops. The induced envelope oscillation is smallest for a point closer to the tail of the bunch where the more rapidly increasing kinetic energy approximately compensates for the decreasing perveance.

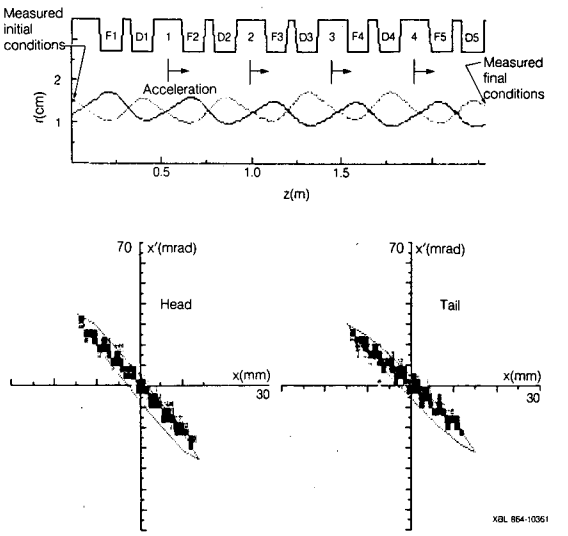

Fig. 1. Behavior of the horizontal and vertical envelopes during acceleration in section A. This K-V calculation begins with measured initial conditions and shows the behavior of the envelopes through five quadrupole periods with acceleration. In the lower part of the figure a comparison is made between the measured final phase space distributions and the calculated K-V ellipses. The quadrupole structure is indicated at the top of the figure "F1", "D1" are the horizontally focussing and defocussing quadrupoles and "1" is the first accelerating gap; the aperture is 2.7 cm.

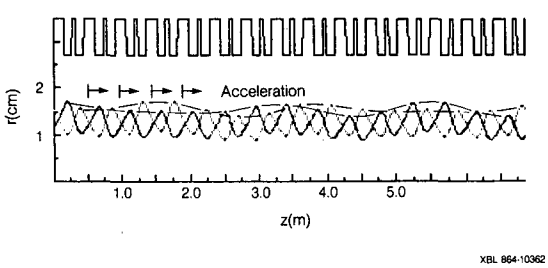

Fig. 2. Development of the envelope oscillation for the middle of the bunch. The horizontal and vertical envelopes are shown for 15 periods with the quadrupole structure indicated at the top of the figure. Also shown are the mismatch oscillations of the maximum horizontal and vertical radii. The first five periods reproduce the acceleration starting with measured initial conditions. The kinetic energy is increased by 10 keV at each of the first four gaps and the current is amplified like $\beta^{1.3}$. The subsequent ten periods show the developed oscillation at constant current, kinetic energy and σ_0.

References

1. C.H. Kim and L. Smith, "Heavy Ion Fusion Half-Year Report," LBL-19501, HI-FAN-285, June 1985.

2. A.I. Warwick, C.H. Kim and T.J. Fessenden, "Heavy Ion Fusion End of the Year Report," LBL-20310, HI-FAN-295, October 1985.

C.M. Celata, L. Smith

The dynamics of a beam with a nonuniform density was studied, (a) for a drifting beam in the focusing system of an accelerator (with either constant or alternating-gradient focusing), (b) for space-charge-limited flow within a diode, and (c) for a single beam created by merging four beams. The case of the beam within the focusing system was investigated using the transverse particle-in-cell simulation code, Shiftxy. The initial distribution function for the beam was taken to be that of a uniform beam plus a density perturbation. The density perturbation took the form of a round spot with a density profile which was either gaussian or uniform. This "hot spot" was used to model density perturbations which might occur in the beam due to nonuniformities in source emission. The case of a gaussian density profile for the entire beam was also studied. The velocity distribution was initially gaussian, with uniform temperature, and the beams were rms matched.

(a) Emittance growth due to the nonuniformity could be accurately calculated using a formula derived by T.P. Wangler[1] and assuming the final state of the beam to be uniform density. The emittance growth occurred, as also seen in Wangler's simulations, in a quarter of a plasma period (see Fig. 1). However, two different behaviors were identified, depending on the magnitude of the initial perturbation. For perturbations where the density of the beam was everywhere greater than approximately half the average density (weak perturbation) the density sloshed in and out of the area of the perturbation throughout the simulation (up to 70 plasma periods, or 200 lattice periods). If the perturbation was stronger than this, the density perturbations damped -- for the case of the gaussian beam, for instance, within about 70 lattice periods. R.C. Davidson has considered these two situations in the study of large amplitude electron plasma oscillations,[2] and the dynamics for beams has been studied analytically recently by O.A. Anderson.[3] These references show that in the case of the weak perturbation, for a cold beam, undamped oscillations at the plasma frequency occur. For the strong perturbation, Anderson has shown that a shock wave results. The large range of frequencies of oscillation resulting from this strong nonlinearity presumably destroys the coherence of the oscillation, as seen in the simulation results.

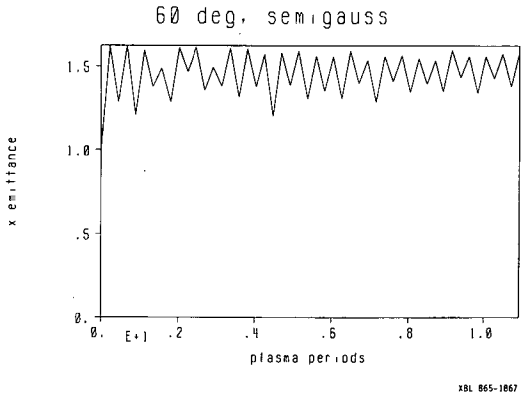

Fig. 1. Emittance growth for an RMS matched beam with velocity profile initially Gaussian. Density perturbation was a centered spot with radius = 0.2 x beam radius, density = 2.7 x beam density. $\sigma_0 = 60°$, constant focusing. RMS equivalent KV beam has $\sigma = 6°$.

(b) Analytical theory was also done to study the evolution of density perturbations close to the source -- in the space-charge-limited-flow region in the diode. A planar diode, infinite in both transverse dimensions, was assumed, and the linearized fluid equations were solved for a steady state for a cold beam. The density used was a uniform density plus a perturbation sinusoidal in the transverse dimensions. For a sinusoidal perturbation in x of wavenumber k, the dependence of the density perturbation on the longitudinal coordinate (z) was found to be:

$$\frac{\Delta n}{n_0} \approx \frac{\Delta J}{J_0} \left| \sum_{t=0}^{\infty} \left[\frac{2}{3} + \frac{1}{6} \sum_{m=1}^{\infty} \frac{\left(\frac{3}{2}\right)! \left(\frac{4}{3}\right)!}{m\left(m + \frac{1}{2}\right)! \left(m + \frac{1}{3}\right)!} \left(\frac{kz}{2}\right)^{2m} \right] \right.$$

This shows that strong growth of small wavelength perturbations takes place within a length in z equivalent to the radius of the diode. For MBE-4, for instance, this is about one third the length of the diode. We therefore conclude that significant evolution of density perturbations due to the source, with the accompanying emittance growth, is likely to occur within the diode. This may account for the factor of approximately 4 above thermal emittance seen in the MBE-4 beams at the entrance to the accelerator. However, quantitative agreement would have to be confirmed by a 3D simulation code.

(c) A study of transverse beam merging has also been started, using the particle-in-cell simulation code. The simulation begins at the time when the beams first "see" each other, and propagates the conglomerate beam through a focusing system within a cylindrical grounded pipe. This can be considered to be another case of a beam with a nonuniform initial density distribution. Simulations show that again the final state is a uniform density beam. Emittance growth occurs both because of phase space dilution and because of the conversion of the electrostatic field energy of the beam into thermal energy when the density profile changes. Preliminary results for the merging of four beams show increases in emittance of between 40 and 250% in both x and y. Emittance growth occurs quickly -- in less than a plasma period.

Finally, various modifications have been made to Shiftxy. The boundary condition of a cylindrical grounded pipe has been added as an option. This can now be used to examine the effect of image forces in the magnetic focusing section of a HIF accelerator. Changes have also been made to allow study of accelerating beams. This will make it possible to discover whether acceleration ameliorates the effect of the emittance growth caused by nonlinearities and image forces for misaligned beams that was reported in previous progress reports.

References

1. T.P. Wangler, K.R. Crandall, R.S. Mills, and M. Reiser, IEEE Trans on Nuc. Sci. 32, 2196 (1985).

2. Ronald C. Davidson, Methods in Nonlinear Plasma Theory, Academic Press, N.Y., 1972, Chapter 3.

3. O.A. Anderson, "Internal Dynamics and Emittance Growth in Non-Uniform Beams," to be published in Particle Accelerators.

NEW DIRECTIONS FOR HIF DRIVERS

E.P. Lee and L. Smith

Introduction

The HIF System Study prompted a re-evaluation of the effect of ion charge state (q) on driver costs. It was found that, at a point along the accelerator of fixed accumulated voltage (not kinetic energy) and employing magnetic focussing, the beam radius, focusing field and pulse duration can be independent of charge state while kinetic energy, electrical current and module power are proportional to charge state. Thus, the desired kinetic energy is achieved in a length shorter by a factor of q with little change in the design of the remaining portion and with increased efficiency because of the increased useful power supplied by each accelerating module. The decrease in cost from ~ 50 MV to final kinetic energy makes higher charge states extremely attractive.

There are potential penalties, however, which have stimulated the lines of investigation discussed below. Because of these problem. We feel that charge state 3 or 4 is probably as far as one should go, with about 16 beams in the main accelerator.

A. Tune Depression

The scaling laws leading to the cost improvements also lead to a more highly depressed tune ($\sigma \sim q^{-3/4}$) for the same emittance, which is dictated by target requirements. In addition the lattice-period should also be changed if charge-state is changed. A systematic study is under way using the transverse simulation code to look for a lower bound on tune, including image effects and coherent oscillations.

B. Final Transport and Focusing

At the end of the accelerator, the electrical current is independent of charge state. Thus the particle current is inversely proportional to z and the required compression ratio increased by the same factor. Also, for the same required particle current, the perveance ($K \propto I_0 q^2/A\beta^2$) is greater by a factor of q^2.

Space charge must be neutralized to a high degree during final transport in a reactor chamber. The neutralization fraction f_e must vary as

$$1 - f_e \propto q^{-2} ,$$

with $f_e \gtrsim .9$ required for typical parameters ($z = 3$). An experimental and simulation study of the available neutralization processes is indicated.

Beam compression in the drift lines between the accelerator and final focus magnets is strongly influenced by the increased perveance of the multiple charged pulse (perveance $\propto I_0 q^2$). On-going simulation efforts in this area (performed in a collaboration with LLNL) are now directed towards the high perveance situation. The points of greatest interest and concern here are the production of useful current wave forms by the compression process and the avoidance of unacceptable growth of longitudinal emittance.

The characteristics of the final focus magnet system are sensitive to the final beam perveance. Experiments and simulation will address the several known sources of beam disturbance in final focus, which result in an enlarged beam spot on the fusion pellet.

Bending of high perveance beams prior to final focus is receiving increased attention. The effects of image forces in combination with a large momentum tilt is being explored with a new code which computes the coupled dynamics of the beam envelope and transverse displacements produced by bends. These effects are expected to be increased in magnitude by increased perveance.

C. Low Energy End

Ion sources in use today produce copious beams at $z = 1$, but production drops off rapidly for higher charge states. We are encouraged, however, by sources currently under development; namely, the Metal Vapor Vacuum Arc (MEVVA) at LBL and similar sources developed by S. Humphries at the University of New Mexico. The production of large currents of multiply-charged metallic ions has been demonstrated, with acceptable emittance.

Recent work (Laslett,Faltens) with $q = 1$, described in this report, has shown that the cost of the low energy ($V < 50$ MV) portion of a driver could be reduced substantially by using a large number of beams (64 or greater). For higher charge states, the low energy end becomes a significant contributor to total accelerator cost and so the feasibility of merging possibly large numbers of beams down to the optimum number for the main accelerator section becomes an important question. This subject is currently being explored in theory and simulation, as well as for possible relevant experiments.

IDENTIFICATION OF ISSUES PERTAINING TO MERGING AND EXPLORATION OF THE MULTIPLE-BEAM PARAMETER SPACE

A. Faltens and L.J. Laslett

It has been evident for several years that the design of a HIF Driver may well require the use of a substantially greater number of multiple beams in the early stages of acceleration than would be appropriate or economically optimum in the later high energy portions of the accelerator (informal notes for a presentation by D. Keefe, dtd. Oct. 22, 1980). The preferential characteristics of heavy ions for target heating and the technological limits to the voltages that can be reasonably assumed for injection result in designs for which the ion velocity at injection and immediately thereafter will be quite small (especially for singly-charged ions). The focusing required for beam transport can be provided effectively under such circumstances by electric-quadrupole focusing, but at higher energies the requisite electric fields become technologically excessive in order to obtain focusing strengths equal to those of attainable magnetic fields. The $\vec{v}\times\vec{B}$ term in the Lorentz force makes the use of magnetic focusing progressively more attractive as energy is increased.

The situation as sketched above thus suggests that the transport of a desired total amount of beam may best be accomplished by the use of a distinctly different number of beams in the low energy portion of an induction linear accelerator, where electrostatic focusing would be employed, than subsequently where magnetic focusing would become appropriate. In the electrostatic regime the technological field-strength restrictions specifically act to limit strongly the envelope dimensions of individual beams, so that the transport of the desired amount of total charge requires the use either of a large number of beams or individual beams of great initial length. The achievable magnetic focusing forces may on the other hand become sufficiently strong at higher energies (especially with use of superconducting magnet windings) that, despite the somewhat greater physical size of magnetic quadrupole structures, a smaller number of larger beams can best be employed to transport the same charge within acceleration cores of substantially the same I.D. as would be used earlier.

The possible necessity, or strong desirability, of merging several beams (e.g., 2 or 4) into one, at one or more locations along a HIF Driver, accordingly has motivated a quantitative review of the foregoing issues. To the degree that such a review, along lines sketched in further detail in the following section, serves to substantiate the desirability of beam merging, so much greater the emphasis that should be devoted within our program to the experimental and analytical investigation of means to achieve such merging -- and of the price that necessarily must then be faced in terms of emittance dilution.

Examples of Multi-Beam Transport

To illustrate the transport issues for a HIF Driver, we have considered the need to accelerate a heavy singly-charged ($A = 209$, $q = 1$) multi-beam array of total charge $n_b\lambda\ell = 300$ μCoulomb. In the early stages of acceleration the kinetic energy is considered to be not substantially greater than that of injection -- namely 3.0 MeV. With the potentials of electrostatic quadrupole electrodes at radius R restricted to lie within $V_{Electrode} = \pm 2.333\times10^6$ R (MKS units), the focusing element occupancy factor in the range $1/2 < \eta < 2/3$, an envelope-to-electrode clearance (R-a) of the order of 1 cm, and a zero-intensity "tune" (phase advance, σ, per period of the transport lattice) $\sigma_o = 75°$, one is led to consider comparatively beams of the various dimensions tabulated in Table I for highly depressed tunes. It will be noted that beams of maximum matched-envelope radius less than that shown for "Case A" would suggest increasingly stringent requirements for alignment, while beams with radii greater than the radius assigned to "Case G" (a = 4.0 cm) would require undesirably great electrode potentials. [The assignment $\sigma_o = 75°$, for which the tabulated value of $\Theta = \sqrt{K}\,L$ applies, may be greater than permissible for a particle centrally situated along a beam bunch under conditions such that a large velocity tilt ($\Delta\beta/\beta$) has developed, but has been adopted provisionally here for purposes of illustration.]

Under the conditions specified for each of the alternative cases, a suitable half period

$$L = \sqrt{\frac{[\text{Kinetic Energy}]/qe}{[V_{Electrode}/R]}}\; R\,\Theta$$

can be evaluated ($\propto \beta$) and the transportable beam intensity (N, λ, & I, per beam) computed -- see Table II. [The quantity p, included in the table, is given by $p = 2.467$ R and represents the transverse period for an electrostatic focusing array similar to the "80% design" used in the MBE-4 device.]

For each such "Case", fixing the characteristics (λ, coulombs/meter) of individual beams, transport of the desired total charge of 300 μCoulomb then dictates a definite value for the product $n_b\ell$ of the number of beams and the length (ℓ) [or duration, $\tau = \ell/(\beta c)$] of the individual beams. It can be desirable to avoid the use of beams of very short duration (e.g., for which τ is less than a few microseconds), since the times spent at the rise and fall of the beam and of the acceleration wave forms could become relatively wasteful. Of greater potential significance in a comparison of configurations with various values of τ is the restriction on permissible acceleration rate that results if one recognizes that some restriction should be placed on the head-tail velocity tilt of a beam passing any fixed location along the accelerator. Such a tilt will necessarily develop shortly after injection (unless the spatial length of the beam is permitted to grow, initially, deferring this problem to a downstream location), and for acceleration with constant ℓ the spatial average of acceleration field is limited to

$$\langle E\rangle = \frac{2}{\ell}\,[\text{Kinetic Energy}/(qe)]\left(\frac{\Delta\beta}{\beta}\right)_{Full}$$

A decreasing bunch length, ℓ, in the electrostatically focused region would require increased electric fields and voltages in the focusing structure, and is not permitted if maximum values are used at injection.

The following tabulation shows possible values, under the conditions mentioned, of ℓ, τ, and $\langle E\rangle$ [for $(\Delta\beta/\beta)_{Full} = 0.20$] for Cases A-G and $n_b = 256, 128, \ldots 16$ beams. Such information can be used to examine in greater detail the configuration of electrode and core assemblies, but it is clear that a capability of accelerating with $\langle E\rangle$ at least in the neighborhood of 0.1 to 0.2 MV/m (in the interest of reduced length for the initial portions of the accelerator) will favor a choice of parameters near the lower left-hand portion of the Table III, for example "Case E", with $n_b = 128$.

For all the cases treated in Table III, the value of $\Phi = \langle E\rangle\tau$ is approximately 0.72 volt-sec/m (neglecting rise and fall times). For cases in which $\langle E\rangle \cong 0.2$ MV/m, the value of $\sqrt{n_b}\,p$ will be found to be close to 1 meter, and provides a rough estimate of the overall transverse dimension of the multi-beam focusing array.

We also are now continuing to examine, for comparative purposes, magnetic-focusing arrays such as will prove suitable at higher ion energies and for which it may well prove to be advantageous to employ a smaller number of beams (e.g., 32 or fewer) that individually are of materially greater radius near the transition point from electric focusing to magnetic focusing.

TABLE I

Transverse Beam Dimensions, Potentials, and Lattice Occupancy Factors for Cases A-G

$\sigma_0 \cong 75°$ and η Various

Case	a (cm)	R-a (cm)	R (cm)	$V_{Electrode}$* (at R) (kV)	V_{Edge} (at a) (kV)	η	Estimated Values	
							Ⓗ	k**
A	0.75	0.85	1.6	± 37.	± 8.2	~ 0.47	1.78	0.134
B	1.0	0.85	1.85	± 43.	± 12.6	1/2	1.72859	0.142
C	1.5	0.9	2.4	± 56.	± 21.87	~ 0.53	1.69	0.152
D	2.0	1.0	3.0	± 70.	± 31.11	~ 0.57	1.64	0.1625
E	2.5	1.0	3.5	± 82.	± 41.7	~ 0.60	1.62	0.169
F	3.0	1.0	4.0	± 93.3	± 52.5	~ 0.63	1.60	0.174
G	4.0	1.0	5.0	± 116.7	± 74.67	2/3	1.56785	0.180

* $V_{Electrode}/R = 2.333 \times 10^6$ V/m.

** The values tabulated for k have been discounted by a few percent, from their respective estimated asymptotic limits. ($k = Q'/u^2$)

TABLE II

Beam Transport Characteristics for Cases A-G

Case	a (cm)	R (cm)	p (cm)	$V_{Electrode}$ (kV)	V_{Edge} (kV)	L (m)	N (ions/m)	λ (Cou/m)	I (Amp)
A	0.75	1.6	3.95	± 37.	± 8.2	0.255 ~ 10.°	3.82×10^{11}	6.12×10^{-8}	0.101
B	1.0	1.85	4.56	± 43.	± 12.6	0.267 ~ 10.5°	6.22×10^{11}	9.96×10^{-8}	0.165
C	1.5	2.4	5.92	± 56.	± 21.87	0.297 ~ 11.7°	1.15×10^{12}	1.85×10^{-7}	0.307
D	2.0	3.0	7.40	± 70.	± 31.11	0.322 ~ 12.7°	1.76×10^{12}	2.81×10^{-7}	0.466
E	2.5	3.5	8.63+	± 82.	± 41.7	0.344 ~ 13.5°	2.45×10^{12}	3.92×10^{-7}	0.649+
F	3.0	4.0	9.87	± 93.3	± 52.5	0.363 ~ 14.3°	3.17×10^{12}	5.08×10^{-7}	0.843-
G	4.0	5.0	12.34	± 116.7	± 74.67	0.3975 ~ 15.65°	4.67×10^{12}	7.48×10^{-7}	1.24

TABLE III

Length and Duration of Individual Beams, and Permissible Average Acceleration Rate, <E>, for $\Delta\beta/\beta = 0.20$

ℓ_0(m)	τ_0(μsec)
<E> (MV/m)	

Case	n_b: 256	128	64	32	16
A	19.16 m 11.56 μs 0.0626 MV/m	38.33 23.12 0.0313	76.65 46.24 0.0157-	153. 92.5 0.00783	307. 185. 0.00391
B	11.8 7.09 0.102	23.5 14.2 0.0510	47.0 28.4 0.0255	94.1 56.8- 0.0128-	188. 114- 0.00638
C	6.34- 3.82 0.189+	12.67 7.64 0.0947	25.3 15.3 0.0474-	50.7 30.6 0.0237	101. 61.1+ 0.0118
D	4.17 2.51 0.288	8.33 5.03 0.144	16.7 10.05 0.0720	33.3 20.1 0.0360	66.7 40.2 0.0180
E	2.99 1.80+ 0.401	5.98 3.61 0.201-	12.0- 7.22 0.100	23.9 14.4 0.0500	47.9 28.9 0.0250
F	2.31- 1.39 0.520	4.61 2.78 0.260	9.22 5.56 0.130	18.4+ 11.1 0.0650	36.9 22.3 0.0325
G	1.57 0.945 0.766	3.13+ 1.89 0.383	6.27 3.78 0.191	12.5 7.56 0.0957	25.1 15.1 0.0479-

MULTIPLE PULSING OF INDUCTION LINACS

A. Faltens

The question of double or multiple pulsing of the induction linac driver was reexamined following T. Godlove's suggestions at the Systems Assessment meeting at EPRI (Oct. 85). The main impediment to multiple pulsing has been and remains a suitable switch which will turn off and recover in the time scale of interest. While a limited amount of work is in progress toward achieving a more ideal switch, we have found substantial advantages in some instances by multiple pulsing with currently existing technology. The cost advantage over the "standard" Palaiseau reference case is in the region of 30%, which makes it the largest single cost reducing item contingent on development uncovered thus far. A preliminary look at combining all of the major cost saving options, such as using higher charge state ions and merging a large number of low energy beams into a smaller number for acceleration at higher energies did not lead to a multiplicative total saving, so it is not clear at this time what the best strategy should be. A particularly attractive feature of the double pulsing scenario is that essentially all of the beam control is demonstrated with the first pulse, which could be followed by installation of the required additional pulsers and beam delay lines for the second pulse.

The induction cores are the most expensive item in a driver at low energies,say, up to 1 GeV, and indirectly keep the acceleration rate low in that region from economic considerations. Taking some given design as a reference point, and keeping everything but the pulse duration fixed, the required volt-seconds in a core are halved if the pulse duration is halved. This corresponds to accelerating the entire charge in two pulses, or double pulsing. The volume of core material required will decrease to between one quarter and one half of the initial core volume, depending on the ratio of the initial outer and inner radii of the core, and lead to substantial savings. The savings are increased if instead of keeping everything else fixed, the cost minimization process of LIACEP is applied to a bunch with one half the initial charge, and "everything" is optimized. The circuit for double pulsing is assumed to be two parallel pulsers driving each induction core and one special reset circuit designed to reset the core between the two beam pulses. At the end of the accelerator, the first pulse must be delayed by the initial interpulse and pulse durations, typically about 20 μsec, and a special bunch compression section must be added at the end of that delay line. The total saving is the difference between the initial accelerator and the cost of the half-charge accelerator plus additional pulsers, delay lines, and compression section. Insofar as two-sided target illumination requires bending of the two clusters of beams in a large arc, some of the delay can be obtained by positioning the reactor chamber asymmetrically in that arc. Repeating this procedure for 3, 4, or more bunch subdivisions results in progressively smaller savings, leading us to concentrate on the double pulse example at this time.

In addition to the paper studies outlined above, we have constructed a double pulse circuit as described. Figure 1 shows the voltages generated by the two acceleration pulsers and the reset pulser between them. Without applying saturating reactors or snubbing circuitry, the thyratron tubes used in the pulsers function as shown up to about 20 kV, whereas in a single pulse mode we usually use them up to about 25 kV, therefore the required derating is tolerable. In this mode of operation the reset voltage adds to the voltage across the second pulser tube, and the second pulse increases the negative voltage across the first pulser. The impedance levels in this circuit were chosen to prevent reapplication of positive voltages to any of the thyratrons in the time interval shown.

In order to keep the thyratrons in the desired safe operating condition during the pulse train, the pulse forming network was mismatched with respect to the load. In the first exercise of driving a resistive load, a 3 ohm pulse line was chosen to drive a 1 ohm load, the 50% reflection ensuring that the reset pulse would not refire the first tube. In the next two exercises of driving actual induction cores, the circuit had to be changed for the particular core and voltage combination desired (because of the very nonlinear behavior of the induction cores) in order to attain the same results. The approximate scaling for the induction cores is that the required switching energy is doubled when the pulse duration is halved; insofar as the volt second product is fixed, the circuit capacity should be halved as the voltage is doubled to generate the shorter pulse. Some additional fine tuning was required to damp the several possible circuit oscillations, but in a short time it was possible to generate flat acceleration pulses of 2, 3, and 4 μsec duration on the induction cores, as well as the initial 5 μsec pulse into a resistive load. In the core driving tests the pulsers drove our entire complement of 6 similar large Metglas induction cores in parallel, therefore the "acceleration voltage" was six times the measured voltage across one core, for example, 36 kV for the 2 μsec pulse duration test as shown in Fig. 2. The single pulse time duration near the injector has been typically 50-100 μsec in the various driver conceptual designs, consequently the 20 μsec gap between the pulses in Fig. 1 is short on that time scale. A variant of double pulsing the entire induction linac is double or multiple pulsing of just the low energy, say, up to 50 MeV portions,and merging the beams either transversely or longitudinally thereafter, analogously to the funneling used by the HIF rf linac designs. The dilutions due to the merging process are being examined at this time. While these various options deviate from the apparent simplicity of a single pulse, straight through system, the cost savings and reduction in buy-in price at the low energies make them very interesting.

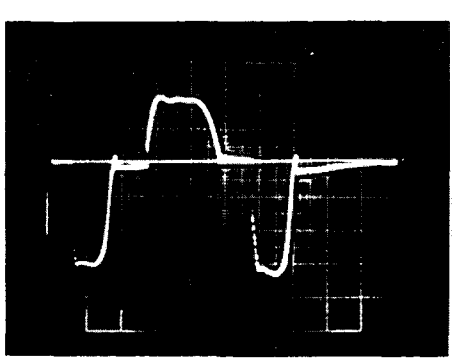

XBB 864-2512

Fig. 1. Double pulsing into a resistive load, where the two negative pulses correspond to 5 μs long, 6 kV amplitude acceleration pulses, and the positive pulse between them corresponds to a "reset" pulse of comparable volt-second area.

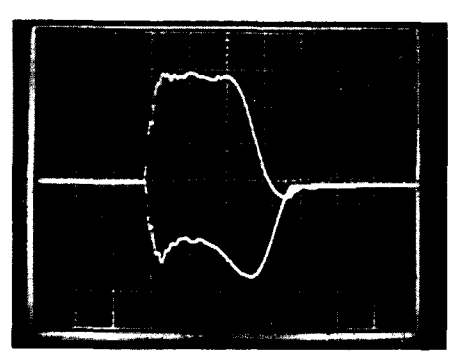

XBB 864-2513

Fig. 2. One of the acceleration pulses of a double pulsing train driving six parallel induction cores. The top trace is the voltage across one core, at 2 kV/div, and the bottom trace is the driving current through that core, at 200 Amps/div. The horizontal scale is 1 μsec/div.

MBE-4 QUADRUPOLE INSULATOR TESTS

C. Pike, G. Stoker

In support of continuing work on the MBE-4 Experiment to accelerate heavy ions to higher energies several quadrupole insulator materials have been tested. These insulators were 4 5/8 inches long and 1 inch in diameter, and were mounted in an MBE-4 quadrupole assembly for testing. Each quadrupole assembly contains four insulators so that four insulators of the same type were tested in each set-up. The present MBE-4 design does not use "flower pots" at the triple point. See LBL-20310, page 9, Fig. 1 for details of quadrupole assembly.

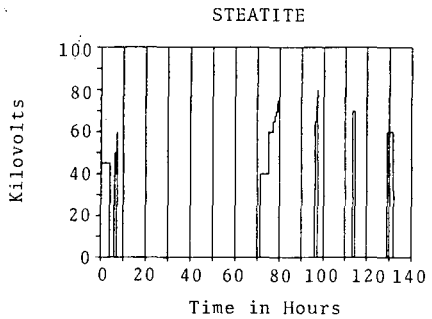

Fig. 1 XBL 864-1531

The tests were made in a vacuum tank with a high voltage feed-thru. The vacuum tank base pressure was about 4×10^{-7} Torr. A 200 kV Spellman power supply was the source of high voltage.

OBJECTIVE: Insulators which can reliably hold 75 kV are required for MBE-4 when the beam energy is about 1 MeV. This test is an attempt to identify the least expensive material which can be used for this purpose.

STEATITE: Insulators were baked at 125°C before installation. Voltage was raised from 45 kV (1st. spark) to 60 kV in about seven (7) hours. Voltage was then raised to 80 kV over a period of two (2) days. Samples sparked continuously at 90 kV with no improvement with time. Samples then would only hold 75 kV before the onset of corona after which the voltage-holding decreased with time. See Fig. 1 for graphed data.

CONCLUSION: These insulators could probably be used at 45 kV to 60 kV as long as they were shielded from the ion beam and secondary electrons.

MACOR: Samples baked to 125°C for one hour. On set of sparking was 25 kV. Reached 80 kV in three (3) hours. After overnight pumping, reached 90 kV in seven (7) minutes and 155 kV in fifteen (15) hours. Overnight pumping resulted in 105 kV to first spark on turn-on and second spark at 115 kV. At 100 kV the leakage or corona current was 100 μa. Further testing resulted in a first spark break-down voltage of 100 kV and 120 kV resulted in a glow discharge. See Fig. 2 for graphed data.

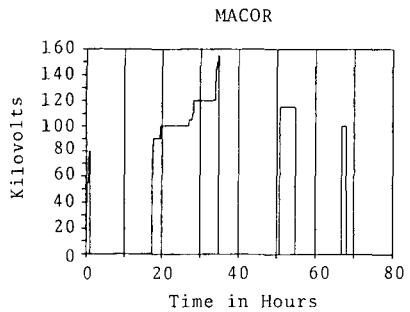

Fig. 2 XBL 864-1532

CONCLUSION: This is probably a good insulator for 75 kV as long as it is shielded from the ion beam and secondary electrons.

ALUMINA (85%): Baked at 125°C for one hour. First spark at 40 kV. Conditioned to 100 kV in about two (2) hours. Glow discharge was noted on ion gauge. Re-X feed-thru insulator was glowing near the ground end. Insulators would continue to come on at 100 kV and go to 120 kV to 130 kV before break down or large leakage current was observed. See Fig. 3 for graphed details.

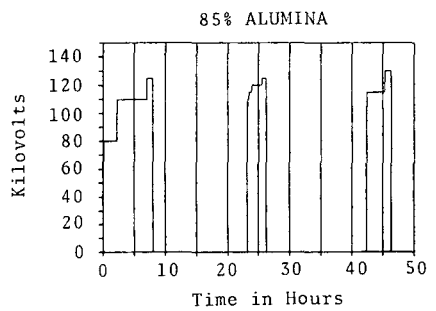

Fig. 3 XBL 864-1533

CONCLUSION: While ultimate withhold voltage was not as high as with the MACOR insulators, this was just about as good. These insulators should work at 50 kV to 75 kV if shielded from the ion beam and secondary electrons.

ALUMINA (97%): NOT BAKED. First spark at 40 kV. Conditioned to 70 kV. Could not condition above 70 kV - 75 kV.

CONCLUSION: All right "just out of the box" for low voltage (50 kV) operation. Try baking.

ALUMINA (97%): Baked at 125°C for one hour. First spark at 45 kV, conditioned up to 100 kV where it sparked or glowed continuously. See Fig. 4 for graphed details.

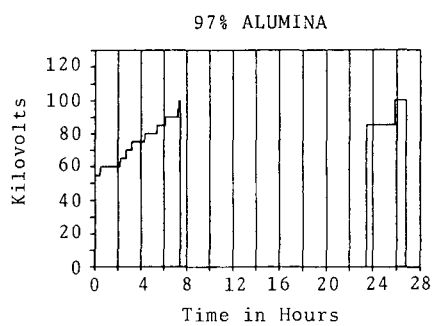

Fig. 4 XBL 864-1534

CONCLUSION: Voltage seemed low compared to unbaked sample and other samples tested.

While previous samples showed some discoloration on the insulator in the last two tests the discoloration was more pronounced. Additional samples of the previously tested samples were tested and all fell short of the reported test values. Further investigation disclosed that an LN trap had gone dry and the system was probably contaminated with oil just prior to testing the first 97% Alumina insulator, hence the last two sets of data probably give too pessimistic a result.

PUBLICATIONS AND INTERNAL NOTES

HI-FAN Notes

HI-FAN-272 LBL-19137	C.H. Kim L. Smith	A Design Procedure for Acceleration and Bunching in an Ion Induction Linac, Particle Accelerators, Vol. 18, pp. 101-113, April 4, 1986.
HI-FAN-297	Denis Keefe	Working Group 3: High-Current Beam Transport AIP San Diego Workshop Proceedings, 139, (San Diego, May 1985)
HI-FAN-298	L. Smith	Chairman's Summary for Working Group on Theory and Simulation for High Current R.F. Accelerators AIP San Diego Workshop Proceedings, 139, (San Diego, May 1985)
HI-FAN-299 LBL-21488A	C.M. Celata L. Smith I. Haber	The Effect of Nonlinear Forces on Transverse Emittance of a Space-Charge-Dominated Heavy Ion Beam Abstract submitted at the 27th Annual Meeting of the Division of Plasma Physics of the American Physical Society, San Diego, CA, Nov. 4-8, 1985.
HI-FAN-300 LBL-18987	L.J. Laslett	Nonlinear Dynamics: A Personal Perspective Proceedings of the Joint US-CERN School on Particle Accelerators, Springer-Verlag, p. 519. (4/86)
HI-FAN-301 LBL-20759	E.P.Lee J. Hovingh A. Faltens	Heavy-Ion Fusion System Assessment Project Quarterly Status Report, Apr.-Jun. 1985
HI-FAN-302 LBL-20760	E.P.Lee J. Hovingh A. Faltens	Heavy-Ion Fusion System Assessment Project Quarterly Status Report, Jul.-Sept. 1985
HI-FAN-303	L. J. Laslett	A-G Beam Transport With Magnetic Focusing in Terms of a Limiting Magnetic Field and with Pronounced Tune Depression. (1/86)
HI-FAN-304 LBL-19508	A. Faltens E.P. Lee S.S. Rosenblum	Beam End Erosion Submitted to the Journal of Applied Physics (3/17/86)

HI-FAN-305	D. Keefe	DOE Energygram, "Increased Beam Intensity for Particle Accelerator Applications," DOE/TIC/EG-85/452, Office of Scientific and Technical Information. (2/86)
HI-FAN-306 LBL-20613	J. Hovingh V.O. Brady A. Faltens E.H. Hoyer E.P. Lee	Cost/Performance Analysis of an Induction Linac Driver System for Inertial Fusion To be published in the Proceedings of the 11th Symposium on Fusion Engineering, Austin, TX, November 18-22, 1985 (2/86)
HI-FAN-307	L.J. Laslett	Multi-Beam Injection Into a Heavy-Ion Induction-Linac Driver with Electrostatic Focusing Employed Initially. (2/86) (a sequel to HI-FAN-303)
HI-FAN-308 LBL-21345a	D. Keefe	Experiments and Prospects for Induction Linac Drivers Abstract submitted to the International Symposium on Heavy Ion Fusion, May 27-29, 1986, Washington, D.C. (3/86)
HI-FAN-309	C. Celata A. Faltens L.J. Laslett E. Lee T. Warwick L. Smith	The HIFAR "Next Step Workshop" (3/86)
HI-FAN-310	E. P. Lee J. Hovingh A. Faltens	HEAVY-ION FUSION SYSTEM ASSESSMENT PROJECT Quarterly Status Report, Oct.-Dec. 1985
HI-FAN-311	A. Faltens	Coherent Betatron Oscillation Phase Shifts (12/4/85)
HI-FAN-313	J. Laslett	Beam Transport Through an Asymmetrical FODO Lattice, and the Potential Instabililty of LLoyd Smith's xy Perturbation. (3/86)
HI-FAN-314 LBL-21346a	E.P. Lee	Accelerator and Final Focus Model for an Induction Linac Based HIF System Study Abstract submitted to the International Symposium on Heavy Ion Fusion, May 27-29, 1986, Washington, D.C. (3/86)

HI-FAN-315 LBL-21347a	D.L. Judd C.H. Kim L.J. Laslett L. Smith A.I. Warwick	Head-to-Tail Velocity Tilt in an Ion Induction Linac Abstract submitted to the International Symposium on Heavy Ion Fusion, May 27-29, 1986, Washington, D.C. (3/86)
HI-FAN-316 LBL-21348a	T.J. Fessenden D.L. Judd D. Keefe C. Kim L.J. Laslett L. Smith A.I. Warwick	Preliminary Results from MBE-4: A Four Beam Induction Linac for Heavy Ion Fusion Research Abstract submitted to the International Symposium on Heavy Ion Fusion, May 27-29, 1986, Washington, D.C. (3/86)
HI-FAN-317 LBL-21349a	C.M. Celata	Simulation of Transverse Merging of Space-Charge-Dominated Beams Abstract submitted to the International Symposium on Heavy Ion Fusion, May 27-29, 1986, Washington, D.C. (3/86)
HI-FAN-318 LBL-21350a	J. Hovingh E.P. Lee A. Faltens V.O. Brady	The Cost of Induction Linac Drivers for Inertial Fusion for Various Target Yields Abstract submitted to the International Symposium on Heavy Ion Fusion, May 27-29, 1986, Washington, D.C. (3/86)

HIFAR Notes (Internal and Informal)

HIFAR-Note-44	Jackson Laslett	Two Addition Waveforms for the I.B.M. PC. (October 28, 1985)
HIFAR-Note-45	C. Kim	MBE-4 Waveform-Update for Sections A & B 12/85
HIFAR-Note-46	C. Kim	MBE-4 Waveforms for Section A & B 12/85
HIFAR-Note-47	D. Vancecek T. Henderson J. Meneghetti	Acceleration Section "B" - Core Detail
HIFAR-Note-48	T. J. Fessenden	A Linear Circuit Model for Magnetic Accelerator Cores (2/13/86)
HIFAR-Note-49	L.J. Laslett	Program ACHAN (2/18/86)
HIFAR-Note-50	L.J. Laslett	Concerning Multi-Quadrupole Half Periods (2/18/86)
HIFAR-Note-51	C. Kim	A Physics Design From 2 MV to 50 MV March 3, 1986
HIFAR-Note-52	L. Smith	Mismatch Oscillations, March 13, 1986
HIFAR-Note-53	L. Smith	g-Factor in MBE-4, (3/14/86)
HIFAR-Note-54	L.J. Laslett	Comments Concerning the Effect of Acceleration Impulses on the Envelope Dimensions of an Extended Beam. (3/86)
HIFAR-Note-55	L.J. Laslett	Some Comments and Illustrative Computations Concerning $\Delta\beta/\beta$ (3/86)
HIFAR-Note-56	C. Kim	Upper Bounds of Velocity Tilt in an Ion Induction Linac. (3/86)
HIFAR-Note-57	T. Fessenden	Towards a Future HIFAR Accelerator Experiment (3/26/86)
HIFAR-Note-58	J. Hovingh	Economic Aspects of Changing Depressed Tune with Energy in 4.24 MJ HIF Driver at Voltages Above 50 MV (3/21/86)
HIFAR-Note-59	J. Hovingh	Economic Aspects of Beam Merging in 4.25 MJ HIF Driver at Voltages above 50 MV (2/28/86)

H.I.F. STAFF ROSTER

Denis Keefe

Robert T. Avery
Donald A. Brodzik
Clarence Chavis
Warren Chupp
Andris Faltens
Thomas J. Fessenden
Bill Ghiorso
David Gough
Wayne Greenway
Edward C. Hartwig
T. Henderson
Ralph Hipple
Cai Houston
Gilbert Jones
Charles H. Kim
Bruce MacDonell
John Meneghetti
Harry Meyer
Chester D. Pike
Tom Purtell
Jim Rice
Stuart Ryce
Gerald L. Stoker
Michael Tiefenback
Bill Tiffany
Mike Towler
David Vanecek
Anthony Warwick

Lloyd Smith

Victor Brady
Christine Celata
David L. Judd
L. Jackson Laslett
Edward P. Lee

William B. Herrmannsfeldt, SLAC

Jack Hovingh, LLNL

H.I.F.A.R. REPORT: DISTRIBUTION LIST

Allied Chemical Corporation

Carl Smith

Argonne National Lab.

Frank T. Cole
Thomas A. Fields
Ronald Martin

University of Arizona

R. Morse

Batelle

John Hartman

Bechtel

W. Allen

BMD/ATC

Milton Hawie

Brookhaven National Lab.

Mark Barton
E. Courant

C.E.A. Bruyeres-le-Chatel

R. Dei-Cas

CEBAF

J. Bisognano
D. Douglas
H. Grunder
C. Leemann

University of Calif., Irvine

Norman Rostoker

Cornell University

John Nation
Ravi N. Sudan

DARPA

Joseph Mangano

Department of Defense (SDIO)

Richard Gullickson
Gerold Yonas

Department of Energy

DP-OIF

Sheldon L. Kahalas
L. Killion
R. Schriever
Marshall Sluyter
Col. Charles Whited

ER

Ryszard Gajewski (AEP)
Terry Godlove (AEP)
Gerry Peters (HENP)
W. Polansky (AEP)
Robert Rader (OPA)
D. Stevens (BES)
David F. Sutter (HENP)
Alvin Trivelpiece, Dir.,
Office of Energy Research
William Wallenmeyer (HENP)

DoE San Office

Rudolf Bredderman
Dennis Neely

E.P.R.I.

Robert Scott

Fermi National Accelerator Lab.

Fred Mills
Lee Teng

F.O.M. Amsterdam

F. Siebenlist

GANIL

P. Lapostolle

GE

John Lucek

GSI

R. Bock
D. Boehne
I. Hofmann

University of Illinois

G. Miley

Institute for Nuclear Study

Y. Hirao

KMS Fusion, Inc.

Alex Glass

Kanazawa University

S. Kawasaki

Lawrence Berkeley Laboratory

D. Atwood, 80/101
R. Avery, 46/189
K. Berkner, 50/149
D. Brodzik, 46/125
C. Celata, 47/112
W.W. Chupp, 47/112
M. Cornacchia, 47/112
T. Elioff, 90/4040
A. Faltens, 47/112
T. Fessenden, 47/112
A. Garren, 47/112
D. Gough, 47/112
E. Hartwig, 47/112
H. Heckman, 50/245
T. Henderson, 46/161
E. Hoyer, 46/187
E. Hyde, 50A/4133E
R. Johnson, 50A/4119
D. Judd, 47/112
D. Keefe, 47/112
C. Kim, 47/112
G. Krafft, 47/112
M. Krebs, 50A/4112
W. Kunkel, 4/230
G. Lambertson, 47/112
L.J. Laslett, 47/112
E.P. Lee, 47/112
E. Lofgren, 47/112
J. Marx, 50/149
J. Meneghetti, 46/161
J. Peterson, 90/4040
A. Sessler, 4/230
D. Shirley, 50A/4133
L. Smith, 47/112
C. Taylor, 46/161
M. Tiefenback, 47/112
D. Vanecek, 58/1011
D. Vaughan, 50/149
A.I. Warwick 47/112

Lawrence Livermore Laboratory

Roger Bangerter, L-477
W. Barletta, L-626
Richard J. Briggs, L-321
John L. Emmett, L-488

Lawrence Livermore Laboratory (cont'd)

Darwin Ho, L-477
John Holzrichter, L-481
William Krupke, L-488
J. Lindl, L-477
Jim Mark, L-477
John Nuckolls, L-477
Louis Reginato, L-526
Erik Storm, L-481

Lockheed

John Siambis

Los Alamos National Laboratory

Ihor Bohachevsky
Richard Cooper
Robert Jameson
Earl Meyer
Roger B. Perkins
Steve Rockwood
Richard Stokes
Tai-Sen Wang
Doug Wilson

University of Maryland

Martin Reiser
Derek Tidman

Max Planck Inst. fur Plasma Physik Garching

Arnulf Schluter

Maxwell Laboratories

Library

National Bureau of Standards

S. Penner
M. Wilson

Naval Research Lab.

Steven Bodner
T. Coffey
Irving Haber
Philip Sprangle
Peter Turchi

Occidental Research Corp.

Wyn Salisbury

Osaka University

T. Mochizuki
C. Yamanaka

Universita di Padova

A. Pascolini
M. Pusterla

Physical Dynamics

G. H. Gillespie

Physics International

Library

Pulse Sciences, Inc.

Ian Smith
Kurt Nielson

RAFAEL

Joseph Shiloh

Rutherford Laboratory

John D. Lawson
Chris Pryor

Sandia Laboratories

Everet H. Beckner
Don Cook
Glenn Kuswa
Tom Martin
J.P. Vandevender

Satori Technology, Inc.

Michael J. Monsler

SLAC

William Herrmannsfeldt, Bin 26
Burton Richter, Bin 7

Soka University

Tetsuya Saito

SOREQ Nuclear Research Center

A. Sternlieb

TRW

J. Gordon
Z. Guiragossian
J. Maniscalco
A.W. Maschke
W. Steele

UCLA

John Dawson

University of Texas at Austin

Toshi Tajima

URA

Edward Knapp

Varian

S.S. Rosenblum

Westinghouse

M. Nahemow
E. W. Sucov

University of Wisconsin

G. Kulcinski
G. Moses
R. Peterson

This report was done with support from the Department of Energy. Any conclusions or opinions expressed in this report represent solely those of the author(s) and not necessarily those of The Regents of the University of California, the Lawrence Berkeley Laboratory or the Department of Energy.

Reference to a company or product name does not imply approval or recommendation of the product by the University of California or the U.S. Department of Energy to the exclusion of others that may be suitable.

LAWRENCE BERKELEY LABORATORY
TECHNICAL INFORMATION DEPARTMENT
UNIVERSITY OF CALIFORNIA
BERKELEY, CALIFORNIA 94720